MIT Libraries | DSpace@MIT

MIT Open Access Articles

Local and long-range functional connectivity is reduced in concert in autism spectrum disorders

Massachusetts Institute of Technology

Local and long-range functional connectivity is reduced in concert in autism spectrum disorders

Sheraz Khan[a,b], Alexandre Gramfort[b,c], Nandita R. Shetty[a,b], Manfred G. Kitzbichler[a,b], Santosh Ganesan[a,b], Joseph M. Moran[d,e], Su Mei Lee[d,e], John D. E. Gabrieli[d,e], Helen B. Tager-Flusberg[f], Robert M. Joseph[g], Martha R. Herbert[a,b], Matti S. Hämäläinen[b,c,e], and Tal Kenet[a,b,1]

Departments of [a]Neurology and [c]Radiology, Massachusetts General Hospital, Harvard Medical School, Boston, MA 02129; [b]A. A. Martinos Center for Biomedical Imaging, Massachusetts General Hospital/Massachusetts Institute of Technology/Harvard University, Boston, MA 02129; [d]McGovern Institute, Massachusetts Institute of Technology, Cambridge, MA 02139; [e]Division of Health Sciences and Technology, Harvard University/Massachusetts Institute of Technology, Cambridge, MA 02139; [f]Department of Psychology, Boston University, Boston, MA 02215; and [g]School of Medicine, Boston University, Boston, MA 02118

Long-range cortical functional connectivity is often reduced in autism spectrum disorders (ASD), but the nature of local cortical functional connectivity in ASD has remained elusive. We used magnetoencephalography to measure task-related local functional connectivity, as manifested by coupling between the phase of alpha oscillations and the amplitude of gamma oscillations, in the fusiform face area (FFA) of individuals diagnosed with ASD and typically developing individuals while they viewed neutral faces, emotional faces, and houses. We also measured task-related long-range functional connectivity between the FFA and the rest of the cortex during the same paradigm. In agreement with earlier studies, long-range functional connectivity between the FFA and three distant cortical regions was reduced in the ASD group. However, contrary to the prevailing hypothesis in the field, we found that local functional connectivity within the FFA was also reduced in individuals with ASD when viewing faces. Furthermore, the strength of long-range functional connectivity was directly correlated to the strength of local functional connectivity in both groups; thus, long-range and local connectivity were reduced proportionally in the ASD group. Finally, the magnitude of local functional connectivity correlated with ASD severity, and statistical classification using local and long-range functional connectivity data identified ASD diagnosis with 90% accuracy. These results suggest that failure to entrain neuronal assemblies fully both within and across cortical regions may be characteristic of ASD.

coherence | parvalbumin

Oscillations in the brain underlie many key cortical functions and coordinate activity between distant brain areas. These rhythmic oscillations are typically studied in distinct frequency bands, often segregated as delta (1–2 Hz), theta (3–7 Hz), alpha (8–12 Hz), beta (13–30 Hz), low gamma (30–60 Hz), and high gamma (>60 Hz). Each frequency band has been associated with specific cognitive and synaptic processes, with some overlaps among bands (1). Substantial evidence indicates that abnormalities in long-range interregional functional connectivity, usually mediated by theta and alpha oscillations, are common in neurodevelopmental disorders (2), including autism spectrum disorders (ASD) (3).

The nature of functional connectivity in ASD has been under intense investigation since the publication of a 2004 report showing reduced long-range functional connectivity in ASD (4). The prevailing hypothesis in the field is that ASD is characterized by reduced long-range functional connectivity and increased local functional connectivity (5–7). The hypothesis that local functional connectivity is increased in ASD is motivated primarily by genetic and histological evidence of reduced neuronal inhibition in ASD (8–10). Although a large body of functional evidence supports the hypothesis of generally reduced long-range functional connectivity in ASD (11), neurophysiological signatures of local functional connectivity in ASD have remained elusive, primarily because noninvasive approaches lack the spatial specificity required to isolate local cortical processes reliably. Testing this hypothesis has been further complicated by the fact that the term "local" is often poorly or vaguely defined in the literature, and has been used to refer to anything from cortical minicolumns (8) to entire cortical lobes (12).

Most studies of local functional connectivity in ASD rely on noninvasive measurements of gamma band synchrony, which is thought to reflect mostly local (up to a few centimeters) cortical processes (13). Several electroencephalography (EEG) and magnetoencephalography (MEG) studies analyzed gamma power at the level of the sensors while participants were at rest or passively heard auditory stimuli, and these studies found both increased and decreased gamma power in individuals with ASD (14–16). These EEG and MEG data were analyzed at the level of the sensors, however, and thus lack spatial specificity because each sensor picks up activity from multiple cortical areas and not necessarily the areas closest to the sensor. It is therefore difficult to assess whether the observed gamma band abnormalities are associated with abnormal local functional connectivity or are, for example, downstream outcomes of earlier or more complex cognitive or sensory processing abnormalities. An alternative is to map data from the EEG or MEG sensors onto the cortex. A series of MEG studies of gamma band responses to simple auditory stimuli (tones and clicks) in ASD used this approach (17–19). Two studies found reduced gamma power at 40 Hz (17, 18), and two found reduced intertrial phase locking in the gamma band (18, 19). Although the findings of reduced gamma power may suggest reduced local functional connectivity in ASD, gamma power measurements might reflect saccadic activity rather than cognitive cortical processes (20). This effect is particularly prominent in the temporal lobe (21), the site of early auditory processing. Because saccades were not monitored in the above studies and ASD individuals have abnormal saccadic activity (22), it is possible that saccadic artifacts contributed to the observed differences. The other main finding, reduced intertrial phase locking in the gamma band, is difficult to link directly to local functional connectivity and may reflect greater variability in response onset, possibly due to subcortical auditory processing abnormalities (23). The hypothesis that local functional connectivity is increased in ASD thus remains prevalent in the field (24, 25).

We sought to measure local functional connectivity using a noninvasive approach that circumvents the limitations and potential confounds associated with using gamma power or phase locking as a proxy for local functional connectivity. We focused on nesting oscillations, in which the phase or amplitude of a lower frequency band modulates the phase or amplitude of a

NEUROSCIENCE

higher frequency band. Nesting of oscillations via phase-amplitude coupling (PAC), where the phase of the lower frequency (usually theta or alpha) modulates the amplitude of the higher frequency (usually beta or gamma), is functionally significant (26), which makes it relevant for evaluating functional connectivity. Importantly, nesting oscillations are believed to reflect mostly local interactions, where local means that the process is confined to a single functionally defined cortical region and occurs on a spatial scale of roughly a centimeter to a few centimeters.

The local nature of PAC has been demonstrated in both human and animal studies. In the first study of theta to high gamma PAC in humans, Canolty et al. (27) used subdural electrodes to show that high gamma amplitude was coupled with theta phase under a variety of tasks and that the degree of coupling was task- and location-dependent. The pattern of PAC in adjacent electrodes, located only 1 cm apart on the surface of the cortex, varied significantly. In a study of the mechanisms underlying PAC, Wulff et al. (28) generated genetically modified mice in which synaptic inhibition was ablated in parvalbumin-positive interneurons. They found reduced local theta power in the hippocampal region of these freely behaving mice. They also found that local theta phase to gamma amplitude PAC was reduced beyond what could be expected from the reduction in theta power alone. This study focused on local coupling between gamma and rat hippocampal theta, but parvalbumin-expressing interneurons are prevalent throughout the human cortex as well (e.g., refs. 29, 30). This putative link between parvalbumin-expressing interneurons and local PAC is particularly relevant in the context of ASD; one study found that parvalbumin-expressing interneurons are underdeveloped in ASD (31), and two different mouse models of autism showed reduced prevalence of these interneurons (32, 33).

PAC is also interesting because it is hypothesized to interact with long-range functional connectivity to integrate information across different spatiotemporal scales of brain networks (34). Local field potential (LFP) and single unit recordings show that hippocampal theta entrains gamma bursts in multiple locations in the neocortex (35) and that spike timing depends not only on local LFP phase but on distant LFP phases and long-range phase coupling (36). One corollary of this hypothesis is that reduced low-frequency (theta or alpha) interregion synchrony should correlate with reduced local PAC. This hypothesis is important for our understanding of the role of oscillations in the cortex in general, and it is particularly relevant for ASD, in which the documented abnormal long-range functional connectivity interactions in the young brain (37) may affect the development and nature of local functional connectivity (38), and vice versa. To date, however, no studies have demonstrated a direct correlation between the strength of long-range coherence and the strength of local PAC.

Given its local nature and important functional role, PAC offers a unique opportunity to study local functional connectivity noninvasively while also examining interactions between local and long-range functional connectivity. Although there have been several noninvasive studies of PAC in humans (e.g., refs. 39, 40), these studies lack spatial specificity. For this study, we used MEG to examine both local PAC and long-range coherence in cortical space in individuals with ASD and typically developing (TD) individuals. We hypothesized that both long-range coherence and local PAC would be reduced in the ASD group, and we further hypothesized that the magnitude of local PAC would be directly proportional to the magnitude of long-range coherence.

We chose to study local and long-range functional connectivity during face processing, a task that is closely related to the core social deficits of ASD (41), and in which abnormalities in long-range functional connectivity in ASD have been documented (42, 43). We recorded MEG data from 17 male adolescents and young adults (aged 14–20 y) with ASD and 20 TD participants while they viewed houses (a nonsocial control stimulus), neutral faces, angry faces, and fearful faces, and we mapped the MEG data from the sensors onto cortical space. We chose to examine task-related rather than resting state functional connectivity because the task activated specific cortical areas and allowed our PAC computations

to focus on a well-characterized and functionally delineated cortical region. Our analysis of local functional connectivity focused on PAC within the fusiform face area (FFA), and our analysis of long-range functional connectivity focused on coherence between the FFA and the rest of the cortex.

Results

Evoked Responses. We delineated the FFA functionally for each individual (Fig. 1A) by contrasting the responses to neutral faces and houses (44) at each vertex of the triangulated cortical surface in the fusiform gyrus. As expected, the evoked responses to houses and neutral faces showed a pattern characteristic of the FFA (45) (Fig. 1B). Responses in the FFA to angry and fearful faces were also indistinguishable within each group of participants (Fig. 1C), so we combined these trials and hereafter refer to the "emotional faces" condition. Although there were also no significant within-group differences in evoked responses to neutral and emotional faces, we kept the neutral and emotional faces conditions distinct for the more complex analyses of long-range and local functional connectivity. There were no group differences in evoked responses in any of the conditions (houses, neutral faces, angry faces, emotional faces).

Long-Range Functional Connectivity. To determine whether there were long-range functional connectivity abnormalities in the ASD group, we computed event-related coherence between the FFA and the rest of the cortex for each participant for all frequencies between 6 Hz and 55 Hz. For each participant and each vertex, we then normalized coherence in the emotional faces condition by coherence in the houses condition (46). The resulting normalized coherence value, called Z-Coherence, is a Z-score of the coherence difference between the houses and emotional faces conditions (46). Statistically significant ($P < 0.05$ corrected) group differences in Z-Coherence were confined to the alpha frequency band (8–12 Hz). These group differences emerged in three distinct cortical regions: a cluster of vertices that overlapped with the left precuneus and whose activity peaked at $t = 150$ ms, a second cluster that overlapped with the left inferior frontal gyrus (IFG) and peaked at $t = 260$ ms, and a third cluster that overlapped with the left anterior cingulate cortex (ACC) and peaked at
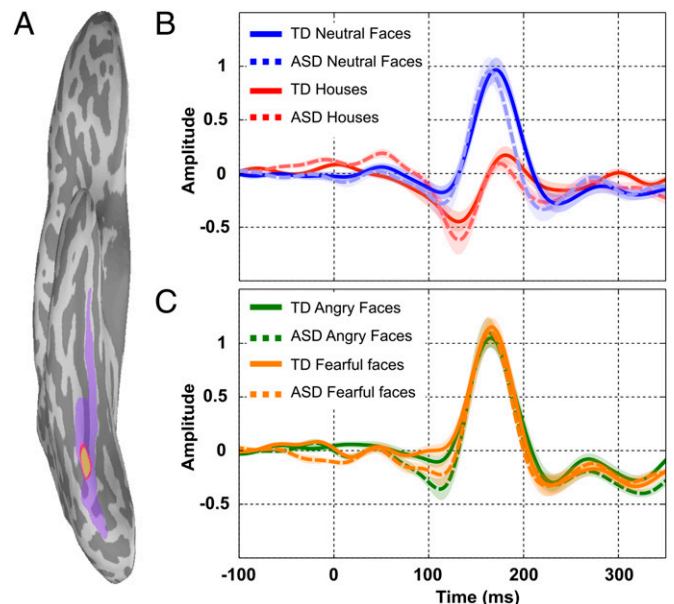

Fig. 1. Evoked responses in the FFA. (A) Functionally determined seed FFA (yellow) in an individual subject. The FreeSurfer fusiform gyrus anatomical label is shaded in purple. (B) Evoked responses to neutral faces and to houses in the FFA. (C) Evoked responses to fearful and angry faces in the FFA. Shaded areas in B and C delineate the standard error (SE).

t = 320 ms (Fig. 2 and Movie S1). For each of these clusters, Z-Coherence was positive in the TD group (greater coherence during emotional faces condition than during houses condition) and negative in the ASD group (lower coherence during emotional faces condition than during houses condition).

These regions align well with prior findings from fMRI studies. Abnormalities in IFG activation and reduced connectivity between the right FFA and the left ACC when viewing neutral faces have been documented in ASD using fMRI (42). Functional connectivity between the right FFA and the precuneus has been shown to emerge in typical individuals when viewing emotional, but not neutral, faces (47). Previous studies of functional connectivity in ASD during face processing used neutral faces only, which probably explains why functional connectivity abnormalities between the FFA and the precuneus have not previously been documented in ASD.

PAC in the FFA. We assessed PAC statistically using the Modulation Index (MI), a score representing the degree of coupling between the phase of one time series and the amplitude of another (27). Specifically, we measured PAC by computing the MI within the FFA for each condition, as well as during the fixation baseline, for each participant.

In both groups, PAC between the alpha band phase and the low gamma band (40–60 Hz) amplitude significantly increased relative to the fixation baseline when viewing houses or faces, as expected, in the visual cortex (48, 49). When viewing faces (neutral or emotional) rather than houses, the TD group had increased PAC between the alpha band phase and low gamma band amplitude, as well as increased PAC between the alpha band phase and high gamma band (75–110 Hz) amplitude ($P < 0.01$ corrected), which was not present during the houses condition (Fig. 3A, *Upper*). There was a trend in the TD group for stronger PAC between the alpha band phase and high gamma band amplitude while viewing emotional, rather than neutral, faces (P = 0.18 corrected).

The ASD group differed from the TD group in two ways. First, the alpha band phase to low gamma band amplitude PAC, which increased in the TD group when viewing faces, remained unchanged in the ASD group. Second, unlike the TD group, there was no emergence of alpha band phase to high gamma band amplitude PAC when viewing faces (Fig. 3A, *Lower*). There were no significant differences between the groups when viewing houses (P = 0.11 corrected) or during fixation. There was no significant group difference in the FFA in either alpha or gamma power in any of the conditions. Group differences in PAC were thus not driven by power differences. As expected (50), group differences in PAC were also not driven by group differences in intertrial coherence (Fig. S1B).
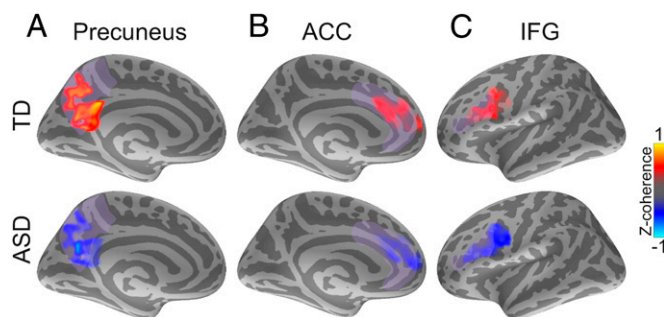

Fig. 2. Coherence for emotional faces normalized by coherence for houses (Z-Coherence), between the FFA and the rest of the cortex for the TD group (*Upper*) and ASD group (*Lower*). The Z-Coherence values shown are masked by the three clusters that showed statistically significant differences ($P < 0.05$ corrected) between the groups (i.e., all values not within these clusters were set to 0). The significant clusters overlap with precuneus (*A*), ACC (*B*), and IFG (*C*) anatomical labels from FreeSurfer (purple shading). For each cluster, the maps are shown at the time of maximal group difference.

Analogous to our Z-Coherence measure, we derived a Z-PAC, defined as PAC during the emotional faces condition normalized by PAC during the houses condition. Z-PAC was significantly lower ($P < 0.03$ corrected) in the ASD group, confirming that PAC between the alpha phase and both low and high gamma amplitudes was significantly reduced in the ASD group relative to the TD group when viewing faces (Fig. 3B).

To verify that our results were confined to the FFA, we conducted a whole-cortex analysis of alpha (8–12 Hz) to high gamma (75–110 Hz) PAC, the frequencies with maximum group differences in PAC in the FFA. This analysis confirmed that the increased PAC was confined to a small area that overlaps with the mean FFA and that only the TD group showed significantly increased PAC in the emotional faces condition relative to the houses condition (Fig. 3C and Figs. S2 and S3). Although outside of the scope of the present study, we also found evidence of increased PAC for houses over faces in the left hemisphere near the occipital pole in the TD group and bilaterally at the occipital pole in the ASD group. This observation may arise from differences between the groups in processing basic visual features of the stimuli, such as spatial frequencies (51).

Correlation Between Local and Long-Range Functional Connectivity. The strength of local cross-frequency coupling within the FFA (Z-PAC) was correlated with the strength of long-range coherence (Z-Coherence) between the FFA and each of the three cortical regions in which we found significant group differences: the precuneus, IFG, and ACC. This correlation between local and long-range functional connectivity measures was significant within each group (Fig. S4) and stronger when data from the two groups were combined (Fig. 4).

Correlations Between Functional Connectivity Measures and Behavioral Measures. To uncover the association between these functional connectivity measures and the ASD phenotype, we first investigated whether they were linked to ASD severity. In the ASD participants, lower Z-PAC values indeed correlated with more severe scores on the social component of the Autism Diagnostic Observation Schedule (ADOS) (Fig. 5A), a behavioral assessment that quantifies the severity of ASD and captures the social impairments of the disorder. We did not find any correlation between ADOS scores and Z-Coherence values.

To determine whether our functional connectivity measures could be used blindly to identify which participants carried an ASD diagnosis, we applied a standard statistical classification procedure, quadratic discriminant analysis (QDA) (52). Our four functional connectivity metrics, Z-PAC (alpha to high gamma) and the three Z-coherence values (for the precuneus, IFG, and ACC), yielded classifier results of 87% sensitivity, 95% specificity, and 90% accuracy for identifying ASD diagnosis (Fig. 5B and Movie S2). We also evaluated the performance of the QDA classifier using subsets of the measures and compared it with a linear discriminant analysis (LDA) classifier. We found that optimal classifier performance required both Z-Coherence and Z-PAC measures and that QDA and LDA performed similarly (Fig. S5).

Discussion

It is well documented that entrainment of neuronal assemblies via long-range coherence is reduced in ASD, and our findings provide further confirmation of this association. Although it is generally believed that local functional connectivity is increased in ASD (5, 24, 25), we found that local functional connectivity was reduced, rather than increased, in ASD. More specifically, our results indicate that local PAC-based functional connectivity in individuals with ASD is identical to that in TD individuals in the absence of a region-specific task. Individuals with ASD failed, however, to increase PAC-mediated local functional connectivity during a more specialized face-viewing task that elicited strong PAC in the FFA in TD individuals.

Although reduced local functional connectivity has not been directly documented in ASD before this study, our results are
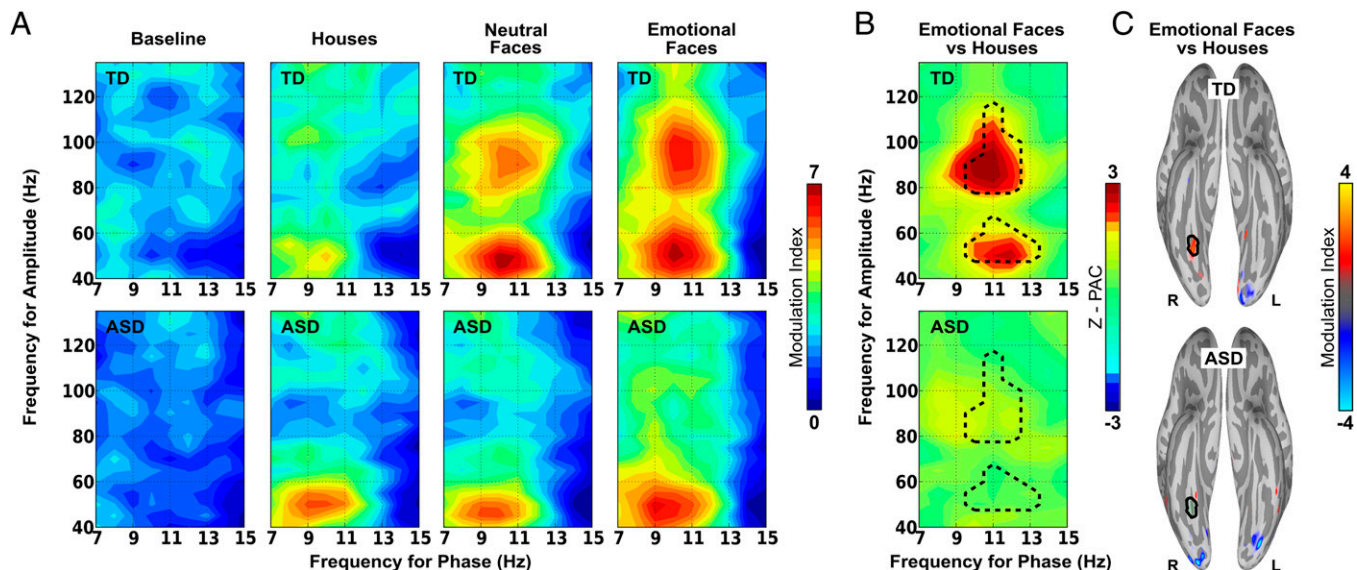
Fig. 3. PAC in the FFA. (*A*) PAC in each condition for each group. (*B*) PAC for emotional faces normalized by PAC for houses (Z-PAC) for the TD group (*Upper*) and ASD group (*Lower*). Dotted lines indicate significant group differences in Z-PAC. (*C*) Z-PAC as in *B* but between alpha and high gamma only, computed over the entire cortex, for each group. The functionally determined FFA is outlined in bold.

consistent with a behavioral tactile study that suggested reduced local functional connectivity in the somatosensory cortex of individuals with ASD (53). Furthermore, a recent structural study found evidence of strongly compromised local structural connectivity in ASD in multiple brain regions (54), which is also consistent with our findings. As mentioned in the introduction, findings of reduced gamma power (17, 18) or phase locking (18, 19), despite potential confounds, also indirectly suggest possible reduced local functional connectivity in ASD. The combination of our current findings, relying on direct measurements of local functional connectivity as mediated by PAC, and these prior studies, which indirectly relate to local functional connectivity using a variety of approaches, suggests that reduced local functional connectivity is likely a prevalent and defining feature of ASD.

Our data are also compatible with histological findings suggesting abnormal and reduced neuronal inhibition in ASD (8–10). Local functional connectivity mediated via PAC or gamma oscillations relies heavily on local inhibitory processes (13, 28). An increased local excitation-to-local inhibition ratio (6) would therefore likely lead to reduced functionally significant local interactions, such as PAC. Our results thus support the hypothesis of reduced local inhibition in ASD. Note that although we see no evidence of increased local excitation in ASD, it is possible that nonfunctionally significant local excitatory interactions are increased in ASD. Because such nonfunctionally significant excitatory interactions would not be

synchronized and would not vary with task demands, however, they would be extremely difficult to assess using noninvasive methods.

We found significant group differences in alpha-gamma PAC in the absence of any significant differences in either alpha power or gamma power within the FFA. This result suggests that the precise timing of gamma bursts, rather than the amount of gamma generated, is abnormal in ASD, at least in this tested scenario. Normal gamma power findings in some ASD studies (16, 19) therefore do not necessarily mean that gamma-mediated local functional connectivity is intact in ASD, because our results show that PAC-mediated local functional connectivity can be reduced even when total power remains the same.

We also found that the normalized strength of local functional connectivity in the FFA, as measured by Z-PAC, was correlated with the normalized strength of long-range functional connectivity between the FFA and three distant cortical regions, measured using Z-Coherence. The absolute nonnormalized PAC and coherence values were not similarly correlated. The correlation between these two spatial scales of functional connectivity suggests that it is unlikely one spatial scale of oscillation-mediated functional interaction would be disrupted while the other remains intact. In other words, abnormalities in long-range cortical functional connectivity likely imply similar abnormalities in local PAC-mediated functional connectivity, and vice versa. Such interactions are probably important in any psychiatric or developmental disorder in which functional connectivity is disrupted, including ASD.
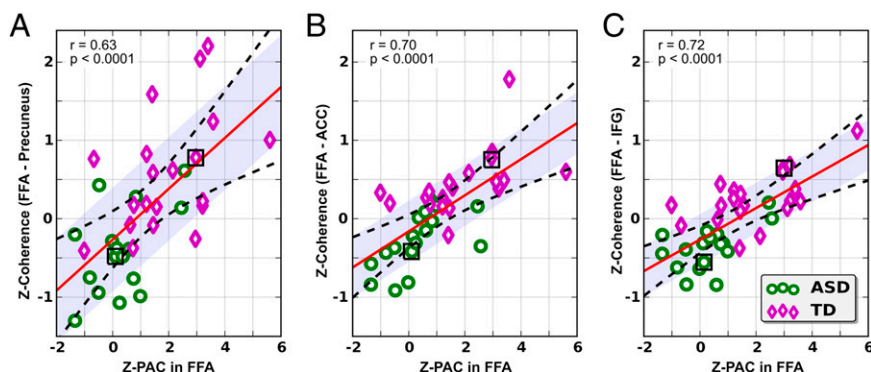

Fig. 4. Mean Z-Coherence value (Fig. 2) between the FFA and the precuneus (*A*), the ACC (*B*), and the IFG (*C*) plotted against the Z-PAC value in the FFA (Fig. 3*B*; alpha phase to high gamma amplitude). The shaded area delineates the SE, and the dashed lines encompass 99% of the confidence interval for correlation. Boxes mark the two participants shown in Fig. S1*A*.
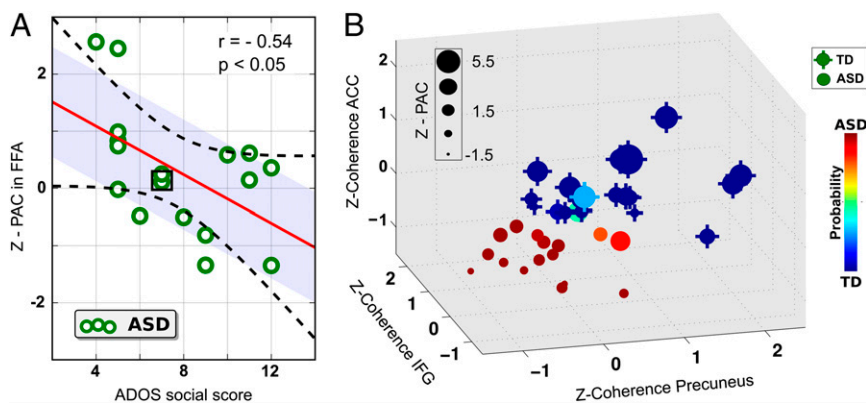
Fig. 5. Correlations between behavioral and neurophysiological data. (*A*) Individual Z-PAC scores are correlated with the social component of the ADOS score. The black box indicates the participant with ASD shown in Fig. S1A. The shaded area delineates the SE, and the dashed lines encompass 99% of the confidence interval of correlation. (*B*) Five-dimensional visualization of QDA analysis using the full dataset: the three Z-Coherence values for the precuneus, ACC, and IFG (the three axes); the Z-PAC (size of marker); and the probability of a participant having a diagnosis of ASD (color of the marker). Plain circles represent the participants with ASD, and crossed circles represent the TD participants.

To date, ASD remains a behaviorally diagnosed disorder despite its clearly biological etiology. We found that ASD severity as measured on the ADOS social subtest was highly correlated with the strength of PAC in the FFA. The ADOS is ASD-specific; thus, this result suggests that reduced PAC, at least during face processing, is likely to be specific to ASD. Furthermore, the combination of local PAC and long-range functional connectivity measures blindly identified participants with ASD with 90% accuracy. These links between our neurophysiological measures and the ASD phenotype suggest that these measures are significant for the etiology of ASD.

In summary, we found that both local functional connectivity indicated by PAC between alpha and gamma bands and long-range functional connectivity quantified by alpha band coherence are reduced in ASD. We also found that these neurophysiological measures are correlated with ASD severity and diagnosis. The magnitudes of local PAC and long-range coherence were directly correlated in both individuals with ASD and TD individuals. Although further studies will be needed to ascertain whether similar abnormalities are present in other cortical areas as well, our results suggest that failure to entrain functionally connected neuronal populations, both local and long range, is characteristic of ASD.

Materials and Methods

Additional details on the materials and methods used in this study are provided in *SI Materials and Methods*.

Participants, Experimental Paradigm, and Data Acquisition. The participants were 17 adolescent and young adult males diagnosed with ASD and 20 age-matched TD males (*SI Materials and Methods*). Informed consent was obtained from all participants. The paradigm presented in the MEG consisted of pictures of houses as well as neutral, fearful, and angry faces (Fig. S6) presented in a randomized block design for 1 s, followed by fixation for 1 s. T1-weighted, high-resolution, magnetization-prepared rapid gradient echo structural images were acquired on a 3.0-T Siemens Trio whole-body magnetic resonance scanner (Siemens Medical Systems) using a 32-channel head coil. MEG data were acquired inside a magnetically shielded room (IMEDCO) using a whole-head Elekta Neuromag VectorView system composed of 306 sensors arranged in 102 triplets of two orthogonal planar gradiometers and one magnetometer. All protocols were approved by the Massachusetts General Hospital (MEG) and Massachusetts Institute of Technology (MRI, behavioral testing) and Boston University (behavioral testing, clinical observation) Institutional Review Boards.

Data Cleaning and Motion Correction. The data were spatially filtered using the signal space separation (SSS) method (55, 56) (Maxfilter software; Elekta Neuromag) to suppress noise generated by sources outside the brain. This SSS procedure also corrects for participants' head motion between runs as well as within each run. The data were epoched into single trials lasting 2 s, extending from 800 ms before stimulus onset to 1,200 ms following it. A total of 48 trials

were collected for each of the four conditions. Epochs were rejected if the peak-to-peak amplitude during the epoch exceeded 150 μV, 1,000 fT, and 3,000 fT/cm in any of the electrooculogram, magnetometer, and gradiometer channels, respectively. This resulted in the loss of 2–8 trials per participant in each condition. To maintain a constant signal-to-noise ratio across conditions and participants, we fixed the number of trials per condition per participant at 40, the minimum number of accepted trials that we had for each condition and participant. For conditions and participants that had more than 40 good trials, we selected the 40 trials randomly. There were no group differences in overall quality of the data, and the number of good (unrejected) trials per condition was not significantly different between groups or across conditions. For each participant, the same set of trials was used for all analyses (delineation of FFA, coherence, and PAC). The MEG data were mapped from the sensors onto a high-resolution cortical surface generated by FreeSurfer (57), using minimum-norm estimate (58) as detailed in *SI Materials and Methods*.

Data Analysis. The FFA was delineated on each individual cortical surface by identifying the vertices within the anatomically defined frontal gyrus that responded more strongly to neutral faces than to houses by contrasting between the two conditions ($P < 0.05$ corrected; Fig. S7). Coherence between the FFA and the rest of the cortex was computed by first averaging the time course across all vertices within the FFA and then computing the event-related coherence (59, 60) between the average FFA time course and each of the other vertices on the cortex, for every frequency between 6 Hz and 55 Hz, using a moving time window of seven cycles per frequency. Using event-related coherence ensured that the induced response did not contribute significantly to the observed coherence differences (Fig. S8). PAC in the FFA was computed using the MI (27) between the frequencies of 7 Hz and 13 Hz for phase and between those of 40 Hz and 130 Hz for amplitude. Global PAC was computed using the same approach between the frequencies of 8 Hz and 12 Hz for phase and between those of 75 Hz and 110 Hz for amplitude. For all analyses, computations were first carried out on single trials and then averaged for each participant and condition.

Statistical Analyses. Cluster-based statistics is a nonparametric, permutation-based method (46, 61) that inherently corrects for multiple comparisons. We used cluster-based statistics with 1,000 permutations for each of our analyses. The test statistics were t tests for the FFA, Z-Coherence (Fig. 2 and Fig. S9), and Z-PAC (Fig. 3 and Fig. S10) comparisons. We used the Wilcoxon rank-sum test for MI comparisons (comparisons across both panels of Fig. 3*B*) because the MI is always positive, and the values were thus not normally distributed. Finally, for statistical computations on the cortex (FFA and Z-Coherence), we computed the connectivity matrix across the vertices using BrainStorm (62).

1. Uhlhaas P, et al. (2009) Neural synchrony in cortical networks: History, concept and current status. *Frontiers in Integrative Neuroscience* 3(17):1–19.
2. Uhlhaas PJ, Singer W (2006) Neural synchrony in brain disorders: Relevance for cognitive dysfunctions and pathophysiology. *Neuron* 52(1):155–168.
3. Uhlhaas PJ, Singer W (2007) What do disturbances in neural synchrony tell us about autism? *Biol Psychiatry* 62(3):190–191.
4. Just MA, Cherkassky VL, Keller TA, Minshew NJ (2004) Cortical activation and synchronization during sentence comprehension in high-functioning autism: Evidence of underconnectivity. *Brain* 127(Pt 8):1811–1821.
5. Belmonte MK, et al. (2004) Autism and abnormal development of brain connectivity. *J Neurosci* 24(42):9228–9231.
6. Rubenstein JL, Merzenich MM (2003) Model of autism: Increased ratio of excitation/inhibition in key neural systems. *Genes Brain Behav* 2(5):255–267.
7. Minshew NJ, Williams DL (2007) The new neurobiology of autism: Cortex, connectivity, and neuronal organization. *Arch Neurol* 64(7):945–950.
8. Casanova MF, Buxhoeveden D, Gomez J (2003) Disruption in the inhibitory architecture of the cell minicolumn: Implications for autism. *Neuroscientist* 9(6):496–507.
9. Fatemi SH, Reutiman TJ, Folsom TD, Thuras PD (2009) GABA(A) receptor downregulation in brains of subjects with autism. *J Autism Dev Disord* 39(2):223–230.
10. Ma DQ, et al. (2005) Identification of significant association and gene-gene interaction of GABA receptor subunit genes in autism. *Am J Hum Genet* 77(3):377–388.
11. Müller RA, et al. (2011) Underconnected, but how? A survey of functional connectivity MRI studies in autism spectrum disorders. *Cereb Cortex* 21(10):2233–2243.
12. Murias M, Webb SJ, Greenson J, Dawson G (2007) Resting state cortical connectivity reflected in EEG coherence in individuals with autism. *Biol Psychiatry* 62(3):270–273.
13. Buzsáki G, Wang XJ (2012) Mechanisms of gamma oscillations. *Annu Rev Neurosci* 35:203–225.
14. Brown C, Gruber T, Boucher J, Rippon G, Brock J (2005) Gamma abnormalities during perception of illusory figures in autism. *Cortex* 41(3):364–376.
15. Orekhova EV, et al. (2007) Excess of high frequency electroencephalogram oscillations in boys with autism. *Biol Psychiatry* 62(9):1022–1029.
16. Braeutigam S, Swithenby SJ, Bailey AJ (2008) Contextual integration the unusual way: A magnetoencephalographic study of responses to semantic violation in individuals with autism spectrum disorders. *Eur J Neurosci* 27(4):1026–1036.
17. Wilson TW, Rojas DC, Reite ML, Teale PD, Rogers SJ (2007) Children and adolescents with autism exhibit reduced MEG steady-state gamma responses. *Biol Psychiatry* 62(3):192–197.
18. Rojas DC, Maharajh K, Teale P, Rogers SJ (2008) Reduced neural synchronization of gamma-band MEG oscillations in first-degree relatives of children with autism. *BMC Psychiatry* 8:66.
19. Gandal MJ, et al. (2010) Validating γ oscillations and delayed auditory responses as translational biomarkers of autism. *Biol Psychiatry* 68(12):1100–1106.
20. Yuval-Greenberg S, Tomer O, Keren AS, Nelken I, Deouell LY (2008) Transient induced gamma-band response in EEG as a manifestation of miniature saccades. *Neuron* 58(3):429–441.
21. Carl C, Açık A, König P, Engel AK, Hipp JF (2012) The saccadic spike artifact in MEG. *Neuroimage* 59(2):1657–1667.
22. Kemner C, Verbaten MN, Cuperus JM, Camfferman G, van Engeland H (1998) Abnormal saccadic eye movements in autistic children. *J Autism Dev Disord* 28(1):61–67.
23. Russo NM, et al. (2008) Deficient brainstem encoding of pitch in children with Autism Spectrum Disorders. *Clin Neurophysiol* 119(8):1720–1731.
24. Wass S (2011) Distortions and disconnections: Disrupted brain connectivity in autism. *Brain Cogn* 75(1):18–28.
25. Vissers ME, Cohen MX, Geurts HM (2012) Brain connectivity and high functioning autism: A promising path of research that needs refined models, methodological convergence, and stronger behavioral links. *Neurosci Biobehav Rev* 36(1):604–625.
26. Canolty RT, Knight RT (2010) The functional role of cross-frequency coupling. *Trends Cogn Sci* 14(11):506–515.
27. Canolty RT, et al. (2006) High gamma power is phase-locked to theta oscillations in human neocortex. *Science* 313(5793):1626–1628.
28. Wulff P, et al. (2009) Hippocampal theta rhythm and its coupling with gamma oscillations require fast inhibition onto parvalbumin-positive interneurons. *Proc Natl Acad Sci USA* 106(9):3561–3566.
29. Bartos M, Vida I, Jonas P (2007) Synaptic mechanisms of synchronized gamma oscillations in inhibitory interneuron networks. *Nat Rev Neurosci* 8(1):45–56.
30. Sohal VS, Zhang F, Yizhar O, Deisseroth K (2009) Parvalbumin neurons and gamma rhythms enhance cortical circuit performance. *Nature* 459(7247):698–702.
31. Anderson WS, Kudela P, Weinberg S, Bergey GK, Franaszczuk PJ (2009) Phase-dependent stimulation effects on bursting activity in a neural network cortical simulation. *Epilepsy Res* 84(1):42–55.
32. Lin FH, et al. (2004) Spectral spatiotemporal imaging of cortical oscillations and interactions in the human brain. *Neuroimage* 23(2):582–595.
33. Gogolla N, et al. (2009) Common circuit defect of excitatory-inhibitory balance in mouse models of autism. *J Neurodev Disorders* 1(2):172–181.
34. Fries P (2005) A mechanism for cognitive dynamics: Neuronal communication through neuronal coherence. *Trends Cogn Sci* 9(10):474–480.
35. Sirota A, et al. (2008) Entrainment of neocortical neurons and gamma oscillations by the hippocampal theta rhythm. *Neuron* 60(4):683–697.
36. Canolty RT, et al. (2010) Oscillatory phase coupling coordinates anatomically dispersed functional cell assemblies. *Proc Natl Acad Sci USA* 107(40):17356–17361.
37. Dinstein I, et al. (2011) Disrupted neural synchronization in toddlers with autism. *Neuron* 70(6):1218–1225.
38. Geschwind DH, Levitt P (2007) Autism spectrum disorders: Developmental disconnection syndromes. *Curr Opin Neurobiol* 17(1):103–111.
39. de Lange FP, Jensen O, Bauer M, Toni I (2008) Interactions between posterior gamma and frontal alpha/beta oscillations during imagined actions. *Front Hum Neurosci* 2:7.
40. Griesmayr B, Gruber WR, Klimesch W, Sauseng P (2010) Human frontal midline theta and its synchronization to gamma during a verbal delayed match to sample task. *Neurobiol Learn Mem* 93(2):208–215.
41. Weigelt S, Koldewyn K, Kanwisher N (2012) Face identity recognition in autism spectrum disorders: A review of behavioral studies. *Neurosci Biobehav Rev* 36(3):1060–1084.
42. Kleinhans NM, et al. (2008) Abnormal functional connectivity in autism spectrum disorders during face processing. *Brain* 131(Pt 4):1000–1012.
43. Bailey AJ, Braeutigam S, Jousmäki V, Swithenby SJ (2005) Abnormal activation of face processing systems at early and intermediate latency in individuals with autism spectrum disorder: A magnetoencephalographic study. *Eur J Neurosci* 21(9):2575–2585.
44. Kanwisher N, McDermott J, Chun MM (1997) The fusiform face area: A module in human extrastriate cortex specialized for face perception. *J Neurosci* 17(11):4302–4311.
45. Deffke I, et al. (2007) MEG/EEG sources of the 170-ms response to faces are co-localized in the fusiform gyrus. *Neuroimage* 35(4):1495–1501.
46. Maris E, Schoffelen JM, Fries P (2007) Nonparametric statistical testing of coherence differences. *J Neurosci Methods* 163(1):161–175.
47. Pantazatos SP, Talati A, Pavlidis P, Hirsch J (2012) Cortical functional connectivity decodes subconscious, task-irrelevant threat-related emotion processing. *Neuroimage* 61(4):1355–1363.
48. Osipova D, Hermes D, Jensen O (2008) Gamma power is phase-locked to posterior alpha activity. *PLoS ONE* 3(12):e3990.
49. Voytek B, et al. (2010) Shifts in gamma phase-amplitude coupling frequency from theta to alpha over posterior cortex during visual tasks. *Front Hum Neurosci* 4:191.
50. Axmacher N, et al. (2010) Cross-frequency coupling supports multi-item working memory in the human hippocampus. *Proc Natl Acad Sci USA* 107(7):3228–3233.
51. Deruelle C, Rondan C, Gepner B, Tardif C (2004) Spatial frequency and face processing in children with autism and Asperger syndrome. *J Autism Dev Disord* 34(2):199–210.
52. Pedregosa F, Varoquaux G, Gramfort A, Michel V, Thirion B (2011) Scikit-learn: Machine learning in Python. *J Mach Learn Res* 12:2825–2830.
53. Tommerdahl M, Tannan V, Holden JK, Baranek GT (2008) Absence of stimulus-driven synchronization effects on sensory perception in autism: Evidence for local underconnectivity? *Behav Brain Funct* 4:19.
54. Shukla DK, Keehn B, Smylie DM, Müller RA (2011) Microstructural abnormalities of short-distance white matter tracts in autism spectrum disorder. *Neuropsychologia* 49(5):1378–1382.
55. Taulu S, Simola J (2006) Spatiotemporal signal space separation method for rejecting nearby interference in MEG measurements. *Phys Med Biol* 51(7):1759–1768.
56. Taulu S, Kajola M, Simola J (2004) Suppression of interference and artifacts by the Signal Space Separation Method. *Brain Topogr* 16(4):269–275.
57. Destrieux C, Fischl B, Dale A, Halgren E (2010) Automatic parcellation of human cortical gyri and sulci using standard anatomical nomenclature. *Neuroimage* 53(1):1–15.
58. Lin FH, et al. (2006) Assessing and improving the spatial accuracy in MEG source localization by depth-weighted minimum-norm estimates. *Neuroimage* 31(1):160–171.
59. Delorme A, Makeig S (2004) EEGLAB: An open source toolbox for analysis of single-trial EEG dynamics including independent component analysis. *J Neurosci Methods* 134(1):9–21.
60. Oostenveld R, Fries P, Maris E, Schoffelen JM (2011) FieldTrip: Open source software for advanced analysis of MEG, EEG, and invasive electrophysiological data. *Comput Intell Neurosci* 2011:156869.
61. Maris E, Oostenveld R (2007) Nonparametric statistical testing of EEG- and MEG-data. *J Neurosci Methods* 164(1):177–190.
62. Tadel F, Baillet S, Mosher JC, Pantazis D, Leahy RM (2011) Brainstorm: A user-friendly application for MEG/EEG analysis. *Comput Intell Neurosci* 2011:879716.